Journal of Construction and Engineering Technology
Journal homepage: www.journal.ferpi.uz

# THERMAL PERFORMANCE COMPARISON OF PCM BASED LATENT HEAT STORAGE SYSTEMS

**Bekzod Abdukarimov[1], Nodirbek Juraboev[2], Mengdi Yuan [2]**

[1]Fergana polytechnic institute, Fergana, Uzbekistan
[2]North China University of Technology, Beijing, China
E-mail: juraboyevnodirbek07091997@gmail.com

## Abstract

The efficient storage and utilization of thermal energy are crucial for advancing sustainable energy systems. Latent Heat Energy Storage Systems (LHESS) leverage the high energy density associated with phase transitions of Phase Change Materials (PCMs), providing an effective solution for thermal energy management. This study focuses on the thermal performance analysis of two different LHESS configurations. Paraffin waxes were selected as a PCM due to their advantageous thermal characteristics, such as high latent heat of fusion, chemical stability, and non-corrosive nature. The research methodology encompasses Computational fluid dynamics LHESS (CFD). Detailed charging and discharging simulations during 30 hours are conducted to predict the thermal performance, efficiency, and operational characteristics of each design under various conditions. The investigation also encompasses a detailed examination of their melting and freezing behavior, thermal conductivity, specific heat and density. Results indicate that at the 30-hour mark, nearly all of the Phase Change Material (PCM) in LHESS 2 has transitioned to the liquid phase when the charging simulation is conducted, whereas approximately 20 percent of the PCM in LHESS 1 remains in the solid phase. During the discharging phase, LHESS 2 demonstrates a faster and more efficient phase transition process. This data suggests that LHESS 2 exhibits a more effective performance compared to LHESS 1. The results are expected to offer valuable insights for optimizing LHESS designs, enhancing their efficiency and sustainability, and guiding the selection of appropriate systems for various industrial and residential applications.

**Keywords:** Latent Heat Energy Storage Systems (LHESS), Phase Change Materials (PCMs), Paraffin Waxes, Thermal Energy Storage.

## 1. Introduction

The escalating global energy demand coupled with the pressing need to reduce greenhouse gas emissions has intensified the exploration and utilization of renewable energy sources. Among these, solar energy stands out due to its abundance and sustainability. However, the intermittent nature of solar radiation necessitates the development of efficient energy storage systems to ensure a continuous and reliable energy supply. Thermal energy storage (TES) systems have become a focal point in this regard, as they enable the capture and storage of excess thermal energy during periods of high solar irradiance for use during times when solar energy is unavailable[1], [2], [3].

Phase Change Materials (PCMs) have emerged as a particularly promising TES technology. PCMs leverage the latent heat of fusion to store and release significant amounts of thermal energy at nearly constant temperatures, offering high energy storage densities and maintaining stable thermal output [4], [5], [6]. PCM-based latent heat storage systems (LHESS) are considered superior to conventional sensible heat storage systems due to their higher energy storage density and efficient thermal management capabilities [7], [8], [9].

The selection of suitable PCMs is critical for the effective design and operation of LHESS. PCMs should exhibit desirable thermophysical properties such as high latent heat, appropriate phase transition temperatures, thermal stability, and compatibility with system materials [10], [11], [12]. Numerous studies have evaluated various PCMs, including paraffin waxes, salt hydrates, and eutectic mixtures, to identify their potential in TES applications [13], [14], [15]. Furthermore, the optimization of system design,

Published online: 8 August 2024
https://doi.org/10.5281/zenodo.13902763
© FarPI Hitech Engineer

including the arrangement of heat exchangers and the enhancement of heat transfer processes, plays a vital role in improving the thermal performance of PCM-based systems [16], [17], [18].

Previous research has extensively examined the thermal behavior and performance metrics of PCM-based TES systems under different operational conditions. For instance, Palacios et al. (2023) analyzed the impact of PCM encapsulation on thermal conductivity and system efficiency, highlighting significant performance improvements [19]. Similarly, Yuzhan et al. (2022) investigated the stability and thermal reliability of salt hydrate-based PCMs, demonstrating their viability for long-term TES applications [20]. These studies provide valuable insights into the factors influencing the performance and reliability of PCM-based LHESS.

## 2. Materials and Methods

### *2.1 Boundary conditions*

Charging simulation of the LHESS was conducted by using the boundary conditions which are given in the Table.2. Inlet velocity of the water is 1l/min and initial and inlet temperatures were 305.15 K and 345.15 K respectively for charging process.

**Table.1**

| Name | Expression | Value | Description |
|---|---|---|---|
| por | 0.1 | 0.1 | Bed porosity |
| $V_{in}$ | 1[l/min] | 1.6667E-5 m³/s | Flow rate |
| T0 | 32[°C] | 305.15 K | Initial temperature |
| Tin | 75[°C] | 345.15 K | Inlet temperature |

The discharging simulation of the LHTESS was performed using the boundary conditions outlined in

**Table.2**

| Name | Expression | Value | Description |
|---|---|---|---|
| por | 0.1 | 0.1 | Bed porosity |
| $V_{in}$ | 1[l/min] | 1.6667E-5 m³/s | Flow rate |
| T0 | 70[°C] | 343.15 K | Initial temperature |
| Tin | 32[°C] | 305.15 K | Inlet temperature |

### *2.2 Governing Equations for simulation.*

(Eq.1, 2, 3, 4) are typically used in LHESS the thermal behavior of PCMs.

Following equation defines a parameter $\alpha_m$which could represent an average or effective value related to the phase change process. $\theta_1$ and $\theta_2$are variables associated with the different phases or states of the material.

$$\alpha_m = \frac{1}{2}\frac{\theta_2-\theta_1}{\theta_1+\theta_2} \quad (1)$$

The next equation indicates that $\theta_1$ and $\theta_2$ are complementary fractions representing the proportions of two phases in the system, such as solid and liquid. Their sum is always equal to 1, indicating the entire system is accounted for.

$$\theta_1 + \theta_2 = 1 \quad (2)$$

Specific heat capacity $C_{p,s}$ of the mixture or system during the phase change is described in the (Eq.3). It is a weighted sum of the specific heat capacities $C_{p,1}$ and $C_{p,2}$ of the two phases, plus a term that accounts for the latent heat $L_{1\to2}$ associated with the phase change, modulated by the temperature derivative of $\alpha_m$.

$$C_{p,s} = \theta_1 C_{p,1} + \theta_2 C_{p,2} + L_{1\to2}\frac{\partial \alpha_m}{\partial T} \quad (3)$$

An effective thermal conductivity $k_s$ of the system as a weighted sum of the thermal conductivities $k_1$ and $k_2$ of the two phases are defined in the (Eq.4).

$$k_s = \theta_1 k_1 + \theta_2 k_2 \quad (4)$$

## 3. Result and discussion.

### *3.1 Charging simulation*

Heat Transfer in Solids and Fluids in COMSOL were utilized to analyze the temperature distribution,

flow patterns within the system. Figure. 2 and Figure. 3 illustrate the temperature variation within LHESS 1, LHESS 2 and the phase change material (PCM) at 15, 20, 25, and 30 hours, respectively. Each sub Figure shows a vertical cross-sectional temperature distribution, with temperatures ranging from 23.4°C to 75°C, as indicated by the color bar.

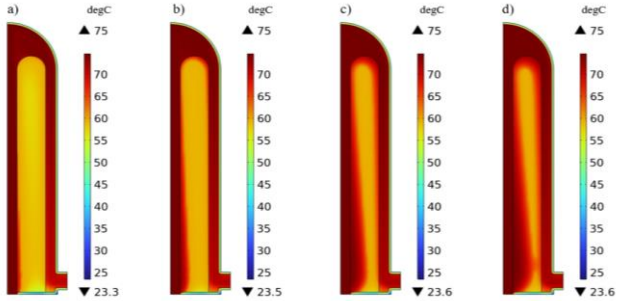



**Fig.1.** Temperature variation of LHESS 1 and PCM at a)15 hours, b)20 hours, c)25 hours, d)30 hours

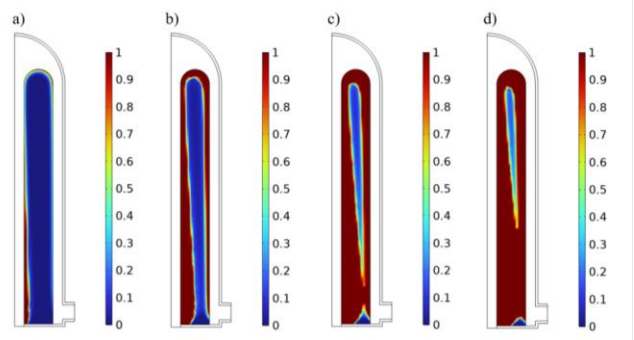



**Fig.2.** Phase transition between phase one and two of the PCM at a)15 hours, b)20 hours, c)25, d)30 hours during charging process in LHESS 1

The PCM shows a significant rise in temperature, with higher temperatures concentrated in the middle section at 15 hours in LHESS 1, while PCM in LHESS 2 exhibits significant heat absorption with higher temperatures concentrated towards the top section, indicating partial phase change initiation see the Figure.2 and Figure.3. The PCM continues to absorb heat, with the temperature gradient extending further downwards, suggesting increased phase transition from solid to liquid state at 20 hours. At 25 hours, a considerable portion of the PCM is now at elevated temperatures, closer to the maximum of 75°C, indicating a more extensive phase transition. The majority of the PCM has reached higher temperatures, nearing complete transition to the liquid state in LHESS 2 comparing to LHESS 1. This is evident as the temperature distribution appears more uniform, with fewer low-temperature regions remaining at 30 hours.

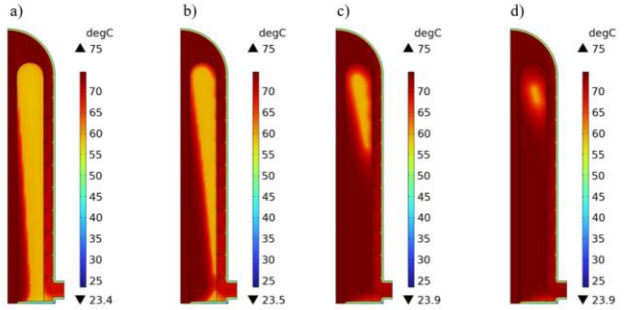



**Fig.3.** Temperature variation of LHESS 2 and PCM at a)15 hours, b)20 hours, c)25 hours, d)30 hours respectively

Figure. 3 illustrates the phase transition occurring between phase one and phase two of the phase change material (PCM) of LHESS 1 LHESS at time intervals of 15, 20, 25, and 30 hours, respectively. During the phase transition energy absorption is increasing when a solid PCM transitions to a liquid state.

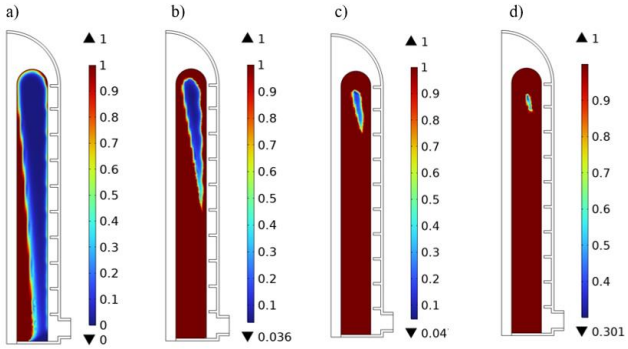



**Fig.4.** Phase transition between phase one and two of the PCM at a)15 hours, b)20 hours, c)25 hours, d)30 hours during charging process in LHESS 2 LHESS

Phase transition process of the phase change material (PCM) in LHESS 2 at intervals of 15, 20, 25, and 30 hours is presented in Fig.4. By the 30-hour mark, nearly the entire PCM in LHESS 2 has transitioned to the liquid state. Conversely, at this same time point, approximately 30 percent of the PCM in LHESS 1 remains in the solid state see the Figure. 3. From these Figures, it can be analyzed that LHESS 2 demonstrated better performance compared to LHESS 1.

### *3.2 Comparative Analysis*

Figure. 5 presents the temperature variation of the Phase Change Material (PCM) at a depth of 0.8 meters during the charging process in both LHESS 1 and LHESS 2. The graph shows how the temperature of the PCM evolves over time, providing insight into the thermal behavior of the material in each LHESS.

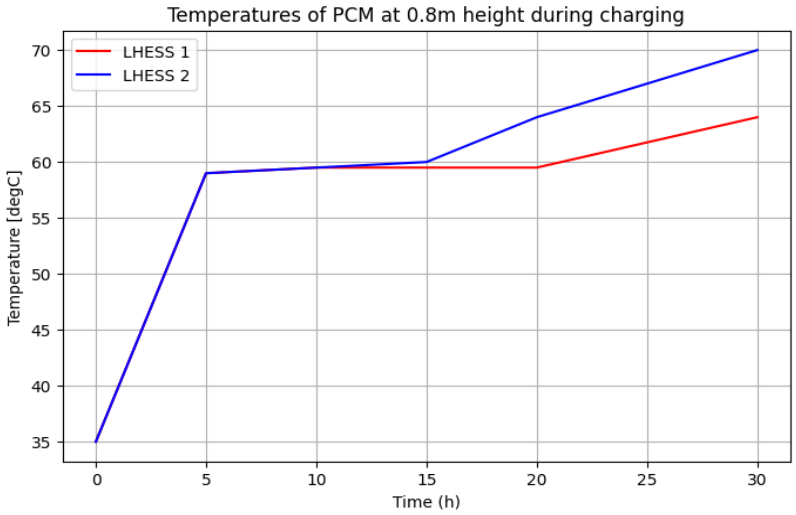



**Fig.5**. Temperature variation of PCM at the point of 0.8m height during charging process in LHESS 1 and LHESS 2.

In LHESS 1, the temperature of the PCM rises rapidly from 35°C to approximately 60°C within the first 5 hours of charging. This rapid temperature increase indicates the initial absorption of sensible heat by the PCM. After reaching 60°C, the temperature curve begins to plateau, with only a marginal increase observed between 5 and 20 hours. This plateau suggests that the PCM in LHESS 1 is undergoing phase change, during which it absorbs latent heat, resulting in minimal temperature variation. By 20 hours, the temperature stabilizes around 60-62°C, indicating that the PCM has reached a thermal equilibrium where further heat absorption is predominantly latent rather than sensible. In contrast, the temperature profile of the PCM in LHESS 2 exhibits a different trend. Similar to LHESS 1, the temperature increases sharply to 60°C within the first 5 hours. However, unlike LHESS 1, the temperature in LHESS 2 continues to rise steadily after 5 hours, albeit at a slower rate. This steady increase continues throughout the intermediate phase (5-15 hours), indicating that the PCM in LHESS 2 is still absorbing heat but at a reduced rate. Notably, after 15 hours, the temperature in LHESS 2 experiences a significant increase, reaching 70°C by the end of the 30-hour charging period. This suggests that the PCM in LHESS 2 has different thermal properties, allowing it to absorb additional sensible heat even after the initial phase change process.

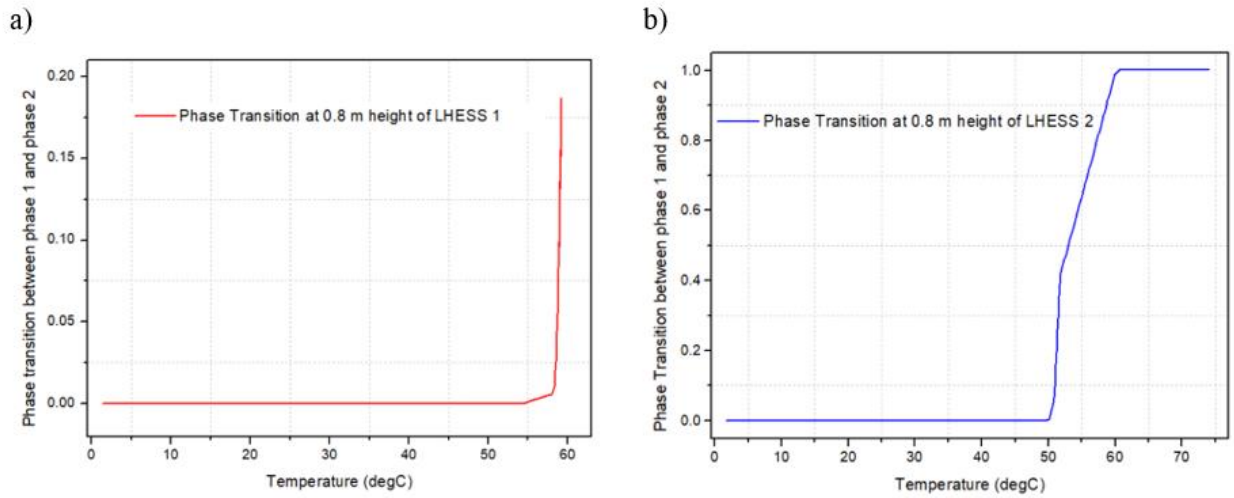



**Fig.6.** Phase transition between phase 1 and phase 2 at the point of 0.8m height during charging process in a) LHESS 1, b) LHESS 2

Figure. 6 illustrates the phase transition from phase 1 to phase 2 of the Phase Change Material (PCM) during the charging process, evaluated at a point of 0.8 meters height in both LHESS 1 and LHESS 2 LHESS. The phase transition is depicted as a function of temperature, providing insights into the thermal

behavior of the PCM in each LHESS. LHESS 1 exhibits a rapid phase transition within a narrow temperature range (55°C to 60°C), indicating a swift phase change. This behavior is typically suitable for applications where quick thermal response is critical. LHESS 2 shows a more gradual phase transition over a wider temperature range (50°C to 65°C), suggesting a slower, more controlled energy storage and release process, which may be beneficial in applications requiring a prolonged thermal response.

### *3.3 Discharging simulation*

Figure.7 and Figure.8 illustrate the phase transition between phase one and phase two of the Phase Change Material (PCM) during the discharging process in two different Latent Heat Energy Storage Systems (LHESS), referred to as LHESS 1 and LHESS 2, respectively. The phase transition is analyzed at four different time intervals: 5, 10, 15, and 20 hours.

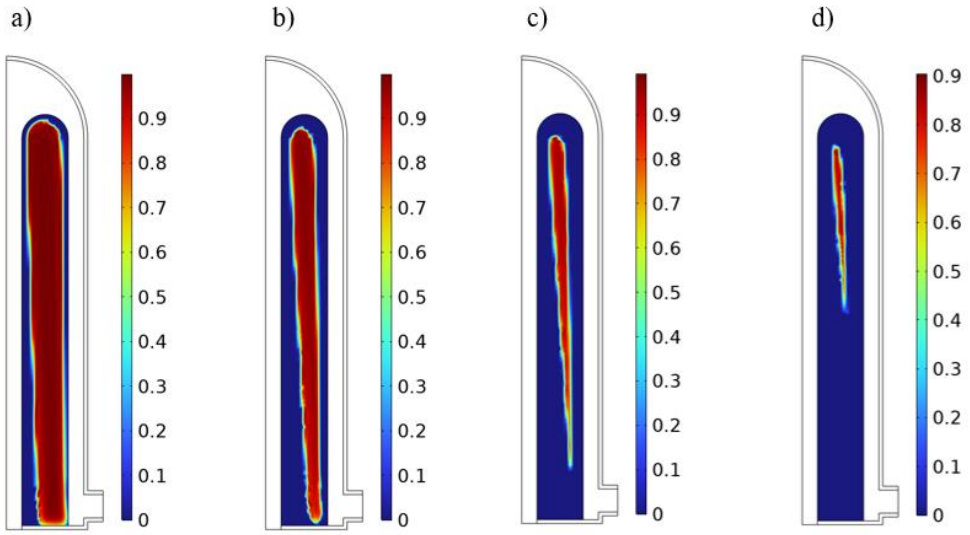



**Fig.7.** Phase transition between phase one and two of the PCM at a) 5 hours, b) 10 hours, c) 15 hours, d) 20 hours during discharging process in LHESS 1.

At 5 hours, the PCM in LHESS 1 begins to undergo phase transition, evident from a narrow region near the boundary where the phase change has started. The majority of the PCM remains in its initial phase, as indicated by the blue color. As the discharging process continues, the transition region expands progressively. By 10 hours, a broader area within the PCM is in the transition phase. At 15 hours, this transition zone has further progressed towards the center of the PCM. Finally, at 20 hours, the phase change has significantly advanced, covering a substantial portion of the PCM, with a distinct boundary between the two phases.

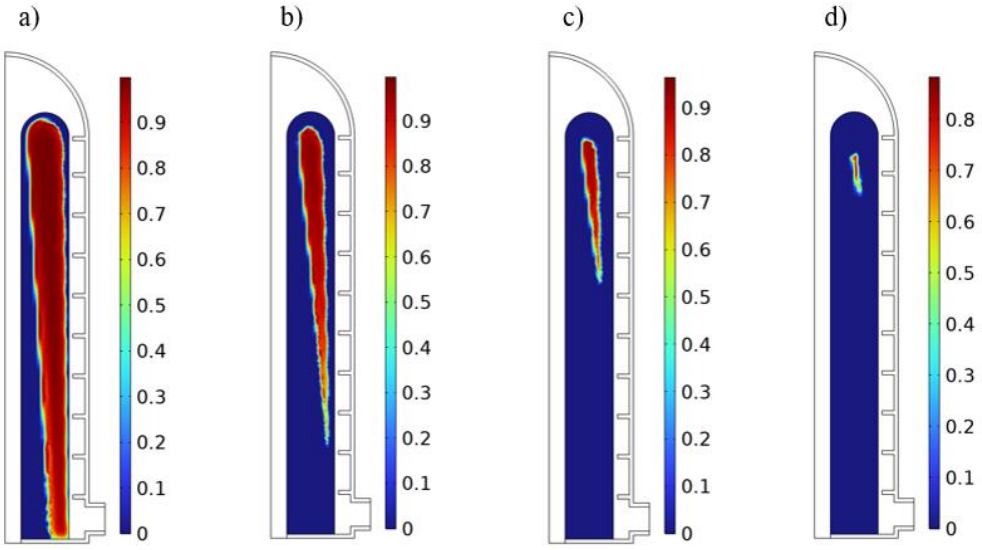



**Fig.8.** Phase transition between phase one and two of the PCM at a)5 hours, b)10 hours, c)15 hours, d)20 hours respectively during discharging process in LHESS 2.

Similarly, in LHESS 2, the PCM starts transitioning at 5 hours, with the initial phase change occurring near the boundary. However, compared to LHESS 1, the phase transition in LHESS 2 advances more rapidly. By 10 hours, the transition region in LHESS 2 is more extensive than in LHESS 1, indicating a more efficient phase change process. At 15 hours, the transition area continues to expand, moving further into the PCM. By 20 hours, LHESS 2 exhibits a more advanced phase transition, with a larger portion of the PCM having transitioned compared to LHESS 1. The comparative analysis between the two LHESSs reveals that LHESS 2 demonstrates a faster and more efficient phase transition process during the discharging phase. At each observed time interval (5, 10, 15, and 20 hours), the phase transition region in LHESS 2 is consistently larger than in LHESS 1. This suggests that LHESS 2 possesses superior thermal management or more effective heat transfer characteristics, leading to a more efficient phase transition of the PCM. These differences could be attributed to variations in design, materials, or operating conditions between the two LHESSs.

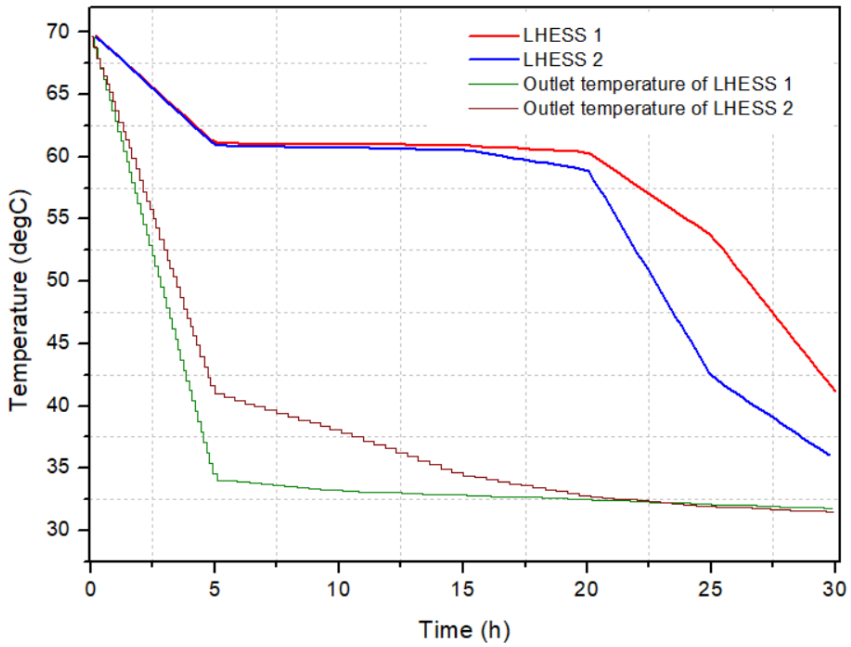



**Fig.9.** PCM and outlet temperature variations at the point of 0.8m depth during discharging process in LHESS 1 and LHESS 2.

Figure.9 compares the temperature variation of PCM at a depth of 0.8 meters during the discharging process in LHESS 1 and LHESS 2. In LHESS 1, the temperature drops sharply from 70°C to 63°C within the first 5 hours, then decreases gradually to 56°C over the next 15 hours. After 20 hours, there is another sharp decline to 42°C by the end of the 30-hour period. This profile indicates a rapid initial cooling, followed by a steady release of energy, and a final phase of significant heat transfer. In LHESS 2, the temperature similarly decreases from 70°C to 62°C within the first 5 hours, followed by a gradual decrease to 58°C over the next 20 hours. After 20 hours, the temperature declines more steadily, reaching 42.5°C by the 25th hour, and then rapidly drops to 36°C by the end of the 30-hour period. Outlet temperature of LHESS 1 significantly decreases to 36°C at 5 hours while outlet temperature of LHESS 2 is declined to 41°C. The temperature at the outlet reached to same points at around 20 hours. This suggests a more controlled release of energy compared to LHESS 1, with a pronounced final temperature drop. Both LHESSs exhibit similar discharging patterns, with LHESS 1 showing a faster energy release in the initial and final stages, and LHESS 2 demonstrating a more gradual and controlled energy release during the plateau phase.

## 4. Model validation

Model comparisons with the experimental results which were carried out by Murray and Groulx, 2014 [23]. The objective of the study is to investigate the phase change behavior of the Phase Change Material (PCM) and to evaluate the thermal performance and efficiency of the cylindrical latent heat energy storage system under practical conditions. Dodecanoic acid is used as Phase Change Material (PCM) see the Table.4. Thermophysical parameters of LHESS and boundary conditions in this article were adapted to the parameters of the LHESS of Murray and Groulx, 2014, and the obtained results were validated against the findings in [23] (Figure. 5). There were computations done for the MAE and the RMSE (Figure. 11).

**Table.3**

| Material properties of Dodecanoic acid | |
|---|---|
| Melting temperature (℃) | 42.5 [℃] |
| Latent heat fusion (kJ/kg) | 182 [kJ/kg] |
| Solid liquid density (kg/m^3) | 869/873 [kg/m^3] |
| Thermal conductivity (kJ/kg℃) | 0.150/0.148 [kJ/kg℃] |
| Solid/liquid specific heat (kJ/kg℃) | 2400/2000 [J/kg℃] |

### *4.1. Finite element analysis*

The Navier Stokes equation in three dimensional with the energy equation was solved using the COMSOL finite element technique. The flow is incompressible and in steady state condition. Water is the circulating fluid at a constant of 0.55 l/min. The formulation used for this model and the boundary conditions can easily be found in reference [23].

*4.1.2. Boundary conditions*

Figure. 10a shows the boundary conditions for the model. At the inlet, the temperature is set at $T_{in}$ and equal to 58 ℃. The initial temperature until 10℃. If the flow rate of the water is equal to 0.55 l/min, inlet velocity of the water should be around $0{,}01\,m/s$ and $0{,}1\,m/s$ . The indicated sections are where the inlet boundary conditions were applied.

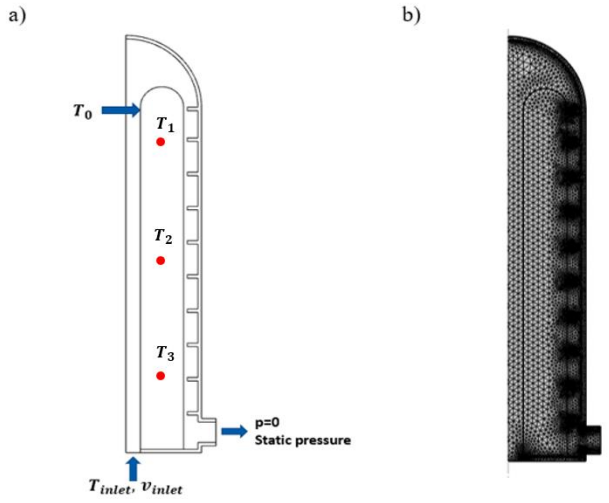



**Fig.10.** a) Boundary condition, b) Generated mesh for the model of LHESS 2

### *4.2. Mesh Resolution Analysis*

A mesh sensitivity analysis was conducted to ensure the accuracy and reliability of the numerical simulations. The final mesh configuration selected for the simulations provided an appropriate level of detail to accurately LHESS the LHESS while maintaining computational efficiency. This mesh sensitivity analysis contributed to the overall robustness and reliability of the simulation results. Number of elements for Mesh controlling is provided in the Table.4 and the calculations were performed using finite element analysis see the Figure.10b.

**Table.5**

| Elements type | Domain elements | Triangles | Quads |
|---|---|---|---|
| Number of elements | 9714 | 8644 | 1070 |

The model's degree of agreement with the observed data was assessed using the mean absolute error (MAE) and standard root means square error (RMSE) to gauge the numerical model's dependability. When the values of the RMSE and MAE are lower, this means that the numerical model's accuracy is higher. These values can be described as shown below:

$$RMSE = \sqrt{\frac{\sum_{i=1}^{n}(P_i - O_i)^2}{n}} \quad (5)$$

$$MAE = \frac{\sum_{i=1}^{n}|P_i - O_i|}{n} \quad (6)$$

where the symbol $P_i$ represents the assessed data point, $O_i$ is the value taken from the simulation, and n signifies the total count or quantity of measured values included within the dataset. Based on equations 8-9 above, RMSE = 4.74, MAE = 4.5 corresponds to the values.

## Conclusion.

Two different Latent Heat Energy Storage Systems (LHESS) were investigated during their charging and discharging operations. For LHESS 2 extruded fins on the inner surface of the TES have been applied.

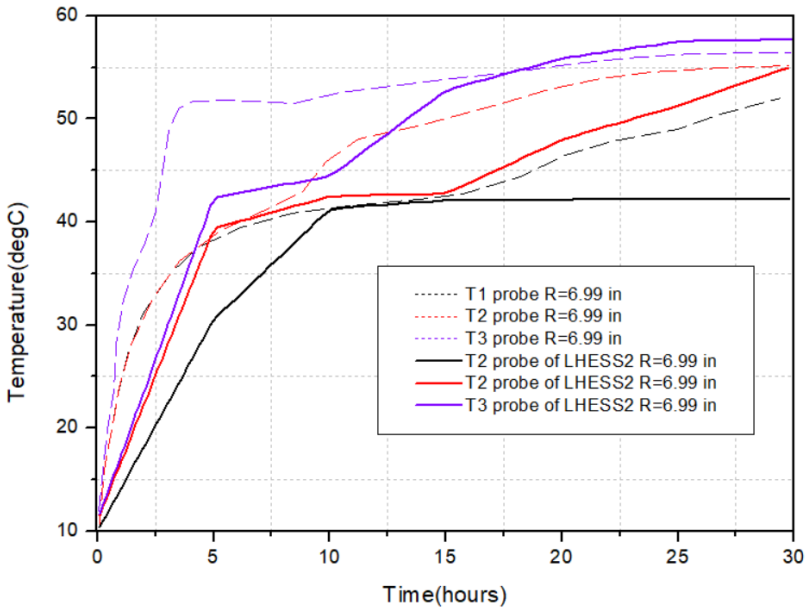



**Fig.11.** Temperature variation of Phase Change Material (PCM) at three different point of LHESS obtained in [23] and LHESS 2.

The simulation results highlight a significant enhancement in thermal performance when utilizing extruded fins on the inner surface of the Thermal Energy Storage (TES) unit. Specifically, the application of extruded fins facilitates improved heat exchange between the heat transfer fluid (HTF) and the paraffin wax, leading to more efficient thermal energy storage and retrieval. Overall, LHESS 2 demonstrates a more rapid and efficient phase transition process during the charging and discharging process. Numerical model of LHESS 2 is validated with the experimental results of Murray and Groulx, 2014 and it was determined that the absolute error was 4.74 and the mean squared error was 4.5. The results serve as a guide for selecting and implementing effective LHESS solutions for various industrial and residential applications, contributing to improved thermal energy management and the advancement of sustainable energy systems.

## REFERENCES


1. L. F. Cabeza, Ed., Advances in thermal energy storage systems: methods and applications, Second edition. Duxford, United Kingdom: Woodhead Publishing, 2021.
2. I. Dincer, A. Hepbasli, A. Midilli, and T. H. Karakoc, Eds., Global Warming: Engineering Solutions. in Green Energy and Technology. Boston, MA: Springer US, 2010. doi: 10.1007/978-1-4419-1017-2.
3. N. Juraboev, "A Comparative Study on Thermal Analysis of Latent Heat Energy Storage Systems Using Phase Change Materials," presented at the ICTEA: International Conference on Thermal Engineering, 2024.
4. M. Kenisarin and K. Mahkamov, "Solar energy storage using phase change materials☆," Renew. Sustain. Energy Rev., vol. 11, no. 9, pp. 1913–1965, Dec. 2007, doi: 10.1016/j.rser.2006.05.005.
5. A. Sharma, V. V. Tyagi, C. R. Chen, and D. Buddhi, "Review on thermal energy storage with phase change materials and applications," Renew. Sustain. Energy Rev., vol. 13, no. 2, pp. 318–345, Feb. 2009, doi: 10.1016/j.rser.2007.10.005.
6. B. Zalba, J. M. Marín, L. F. Cabeza, and H. Mehling, "Review on thermal energy storage with phase change: materials, heat transfer analysis and applications," Appl. Therm. Eng., vol. 23, no. 3, pp. 251–283, Feb. 2003, doi: 10.1016/S1359-4311(02)00192-8.
7. M. M. Farid, A. M. Khudhair, S. A. K. Razack, and S. Al-Hallaj, "A review on phase change energy storage: materials and applications," Energy Convers. Manag., vol. 45, no. 9–10, pp. 1597–1615, Jun. 2004, doi: 10.1016/j.enconman.2003.09.015.
8. H. Mehling and L. F. Cabeza, Heat and cold storage with PCM: An up to date introduction into basics and applications. in Heat and Mass Transfer. Berlin, Heidelberg: Springer Berlin Heidelberg, 2008. doi: 10.1007/978-3-540-68557-9.
9. Solar Heat Storage: Volume I: Latent Heat Material. CRC Press, 2018. doi: 10.1201/9781351076753.
10. X. Xiao, P. Zhang, and M. Li, "Preparation and thermal characterization of paraffin/metal foam composite phase change material," Appl. Energy, vol. 112, pp. 1357–1366, Dec. 2013, doi: 10.1016/j.apenergy.2013.04.050.
11. S. Mondal, "Phase change materials for smart textiles – An overview," Appl. Therm. Eng., vol. 28, no. 11–12, pp. 1536–1550, Aug. 2008, doi: 10.1016/j.applthermaleng.2007.08.009.
12. B. Yang, J. Liu, Y. Song, N. Wang, and H. Li, "Experimental study on the influence of preparation parameters on strengthening stability of phase change materials (PCMs)," Renew. Energy, vol. 146, pp. 1867–1878, Feb. 2020, doi: 10.1016/j.renene.2019.08.052.
13. A. F. Regin, S. C. Solanki, and J. S. Saini, "Heat transfer characteristics of thermal energy storage system using PCM capsules: A review," Renew. Sustain. Energy Rev.,

vol. 12, no. 9, pp. 2438–2458, Dec. 2008, doi: 10.1016/j.rser.2007.06.009.

14. X. Py, R. Olives, and S. Mauran, "Paraffin/porous-graphite-matrix composite as a high and constant power thermal storage material," Int. J. Heat Mass Transf., vol. 44, no. 14, pp. 2727–2737, Jul. 2001, doi: 10.1016/S0017-9310(00)00309-4.
15. D. O. Akamo et al., "Enhanced thermal reliability and performance of calcium chloride hexahydrate phase change material using cellulose nanofibril and graphene nanoplatelet," J. Energy Storage, vol. 75, p. 109560, Jan. 2024, doi: 10.1016/j.est.2023.109560.
16. F. Agyenim, P. Eames, and M. Smyth, "A comparison of heat transfer enhancement in a medium temperature thermal energy storage heat exchanger using fins," Sol. Energy, vol. 83, no. 9, pp. 1509–1520, Sep. 2009, doi: 10.1016/j.solener.2009.04.007.
17. L. Fan and J. M. Khodadadi, "Thermal conductivity enhancement of phase change materials for thermal energy storage: A review," Renew. Sustain. Energy Rev., vol. 15, no. 1, pp. 24–46, Jan. 2011, doi: 10.1016/j.rser.2010.08.007.
18. A. Abhat, "Low temperature latent heat thermal energy storage: Heat storage materials," Sol. Energy, vol. 30, no. 4, pp. 313–332, 1983, doi: 10.1016/0038-092X(83)90186-X.
19. A. Palacios, M. E. Navarro-Rivero, B. Zou, Z. Jiang, M. T. Harrison, and Y. Ding, "A perspective on Phase Change Material encapsulation: Guidance for encapsulation design methodology from low to high-temperature thermal energy storage applications," J. Energy Storage, vol. 72, p. 108597, Nov. 2023, doi: 10.1016/j.est.2023.108597.
20. Y. Li et al., "Stable salt hydrate-based thermal energy storage materials," Compos. Part B Eng., vol. 233, p. 109621, Mar. 2022, doi: 10.1016/j.compositesb.2022.109621.
21. Physical-technical institute, Academy of Sciences of Uzbekistan, J. Akhatov, K. Akhmadov, N. Juraboyev, and Physical-technical institute, Academy of Sciences of Uzbekistan, "Thermal performance enhancement in the receiver part of solar parabolic trough collectors," UNEC J. Eng. Appl. Sci., vol. 3, no. 2, pp. 5–13, Dec. 2023, doi: 10.61640/ujeas.2023.1201.
22. I. Jmal and M. Baccar, "Numerical study of PCM solidification in a finned tube thermal storage including natural convection," Appl. Therm. Eng., vol. 84, pp. 320–330, Jun. 2015, doi: 10.1016/j.applthermaleng.2015.03.065.
23. R. E. Murray and D. Groulx, "Experimental study of the phase change and energy characteristics inside a cylindrical latent heat energy storage system: Part 1 consecutive charging and discharging," Renew. Energy, vol. 62, pp. 571–581, Feb. 2014, doi: 10.1016/j.renene.2013.08.007.